



**HAL**  
open science

## Evaluation of drag coefficient for a quadrotor model

Gautier Hattenberger, Murat Bronz, Jean-Philippe Condomines

► **To cite this version:**

Gautier Hattenberger, Murat Bronz, Jean-Philippe Condomines. Evaluation of drag coefficient for a quadrotor model. 13th International Micro Air Vehicle Conference, Sep 2022, Delft, Netherlands. pp.39–46. hal-03859308

**HAL Id: hal-03859308**

**<https://enac.hal.science/hal-03859308>**

Submitted on 6 Dec 2022

**HAL** is a multi-disciplinary open access archive for the deposit and dissemination of scientific research documents, whether they are published or not. The documents may come from teaching and research institutions in France or abroad, or from public or private research centers.

L'archive ouverte pluridisciplinaire **HAL**, est destinée au dépôt et à la diffusion de documents scientifiques de niveau recherche, publiés ou non, émanant des établissements d'enseignement et de recherche français ou étrangers, des laboratoires publics ou privés.

# Evaluation of drag coefficient for a quadrotor model

Gautier Hattenberger, Murat Bronz and Jean-Philippe Condomines  
 ENAC, Université de Toulouse, France  
 firstname.lastname@enac.fr

## ABSTRACT

This paper focuses on the quadrotor drag coefficient model and its estimation from flight tests. Precise assessment of such a model permits the use of a quadrotor as a sensor for wind estimation purposes without the need for additional on-board sensors. Firstly, the drag coefficient has been estimated in a controlled environment via wind generator and motion capture system. Later, the evolution of the coefficient is observed for various mass and fuselage shapes. Finally, an estimation method is proposed, based on the least-squares optimization, that evaluates the drag of the quadrotor directly from outdoor flight data. The latter leads the methodology towards an easier adoption in other researchers' systems without the need for complex and expensive flight testing facilities. The accuracy of the proposed method is presented both in simulation, based on a realistic flight dynamics model, and also for real outdoor flights.

## 1 INTRODUCTION

Wind field measurement is an important aspect of atmospheric science. Especially, boundary-layer meteorology requires wind speed and direction to study the atmospheric processes close to the ground surface. The ideal would be the use of multiple sensor bases capturing the wind information with high spatial and temporal resolution. However, this solution is practically not feasible from the cost and logistics point of view. The use of UAVs has a big impact on this point, and therefore several methods have already been investigated by researchers. A very common way is to use a fixed-wing aircraft and estimate the wind from the flight track [1] or with the help of additional sensors mounted onto the system, such as a multi-hole probe [2, 3] or even a cheaper solution based on a combination of the simple Pitot tube and wind-vanes [4].

On the other hand, the multi-rotors, known as drones, can offer operational easiness over fixed-wing vehicles as they can take off and land vertically within a confined space and be more compact. However, being an often underactuated system, they have to incline towards the desired direction, which is becoming inappropriate for some of the sensors used in fixed-wing vehicles. Additionally, the flight speed of multi-rotors is typically lower compared to fixed-wing vehicles, lowering the dynamic pressure and making it difficult to use

multi-hole probes. Hence, [5] compared the use of four different anemometers on a quadrotor. The study revealed that a thermal anemometer could be used, at the cost of modifications to the UAV structure to place it far enough from the disturbances induced by propellers.

The compactness of the multi-rotors can be used as an advantage, and instead of using additional sensors, the motion and attitude of the vehicle can reveal information about the wind speed and direction [6, 7, 8, 9]. Gonzalez et.al. [7] present different possible models such as static, kinematic, or full dynamic. In addition, a methodology to extract the required parameters is given. They have characterized the propulsion system by using a motor test bench during a wind tunnel experiment, and the drag is extracted from outdoor flights at constant ground speed in steady air. The drag is observed to be proportional to the relative airspeed. Schiano et.al [6] and Marino et.al [10], used experiments with a six-axis force balance, a very precise but fragile and expensive system. Finally, [8] presents a nonlinear observer able to accurately predict the wind components, using only low-cost Inertial Measurement Unit (IMU) and ground speed measurements. The drag force is considered proportional to the rotational speed of the motors, which is almost constant during operation, leading to a constant rotor drag coefficient, similar to [7, 11]. Outdoor flights have been performed in [9, 7] and comparison between ground reference measurements are made, showing the feasibility of wind measurement from quadrotors based on IMU and GPS measurements. Note that estimating the vertical components of the wind requires an accurate modeling of the propulsion system and despite that, have not shown satisfactory results in [12].

In the light of these general principles and authors' previous work [13], the present article is organized as followed. First, the problem modeling focuses on the equations of motion, the hypothesis, and limitations, as well as the experimental airframe. Then, the parameter identification method and evaluation of the mass and fuselage shape effect are presented. Finally, simulation and outdoor flight experiments are described and their results are analyzed.

## 2 PROBLEM FORMULATION

The objective of this study is to estimate the drag coefficient and evaluate the effect of various physical characteristics, such as mass and shape. This section is presenting the dynamic models and the experimental setup that will be used.

### 2.1 Kinematic and aerodynamic model

The kinematic model is the same than a previous work [13] and is very common in the literature [7]:

$$\dot{\mathbf{X}} = \mathbf{V}_k = \mathbf{V}_r + \mathbf{V}_w \quad (1)$$

$$m\dot{\mathbf{V}}_k = m\mathbf{g} + \mathbf{D}(V_a) + \mathbf{T} \quad (2)$$

where:

- $\mathbf{X}$  is the position vector relative to earth frame
- $\mathbf{V}_k$  is the ground speed vector relative to earth frame (inertial velocity)
- $\mathbf{V}_r$  is the relative air speed vector
- $\mathbf{V}_w$  is the wind speed vector relative to earth frame
- equation 1 represents the wind triangle
- $m$  is the mass of the model and  $\mathbf{g}$  the gravity vector
- $V_a = \|\mathbf{V}_r\|$  is the norm of the airspeed
- $\mathbf{D}$  is the drag vector in earth frame, as a function of airspeed
- $\mathbf{T}$  is the control forces vector (thrust) in earth frame

The wind speed is supposed to be constant or slowly varying, therefore the derivative of the wind triangle (equation 1) gives:

$$\dot{\mathbf{V}}_w = 0 \Rightarrow \dot{\mathbf{V}}_k = \dot{\mathbf{V}}_r \quad (3)$$

The drag modeled as a linear function of the relative airspeed:

$$\|\mathbf{D}\| = k V_a \quad (4)$$

where  $k$  is a constant factor determined with a calibration method or estimated from flight data. The drag is usually quadratic with the airspeed, however the influence of the rotor drag at low speed results in a nearly linear drag [13, 12, 11]. The validity of this model is also discussed in section 3.2.

The control force vector  $\mathbf{T}$  can be expressed from the norm of the thrust  $T_{total}$  and the orientation of the body relative to earth frame represented by the rotation matrix  $\mathbf{R}_{0b}$ . This matrix can be computed from Euler angles  $\phi$ ,  $\theta$  and  $\psi$  with the classic DCM matrix as in [7].

$$\mathbf{T} = \begin{pmatrix} T_x \\ T_y \\ T_z \end{pmatrix} = \mathbf{R}_{0b} \begin{pmatrix} 0 \\ 0 \\ T_{total} \end{pmatrix} \quad (5)$$

In practice, the total thrust is computed from the assumption that the vertical acceleration is null and that the projection of the thrust on the vertical axis is equal to the mass of the drone, resulting in the following formula:

$$T_{total} = \frac{mg}{\cos \phi \cos \theta} \quad (6)$$

### 2.2 Experimental setup

The custom quadrotor frame presented in [13] have been reused for this experiment. It is a simple cross shape made of thin aluminum bars to hold the motors and it is possible to place a spherical 3D-printed central body around the electronic components and the battery. In the previous work, the spherical body was always used. Since the goal of this new work is to study the influence of mass and shape, several experiments are conducted with different configurations. Starting from the the base configuration, additional masses can be added to increase the weight with changing the overall shape (thus, not changing noticeably the friction drag) or by adding the spherical body over the central part. Since the maximum additional mass that can be added is almost the same than the frame with the sphere, we consider that it allows to compare the quadrotor with the same mass condition but with a different shape. The Figure 1 is presenting the different elements: base frame, extra masses and spherical body.

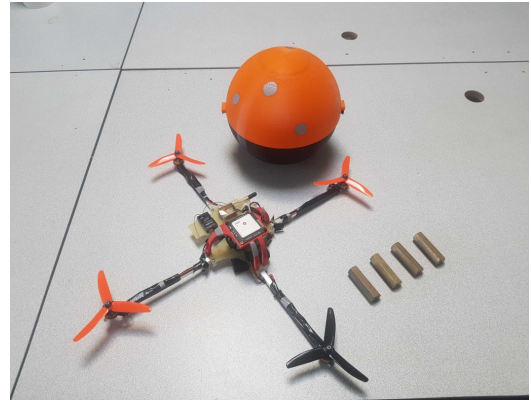


Figure 1: Quadrotor with additional masses and custom spherical body.

The general characteristics and components are summarized in the Table 1. The autopilot software used is the *Parrot* UAV System [14]. For indoor calibration and experiments, the localization is provided by a motion capture system from *Optitrack*. For outdoor flights, a GPS receiver is used.

## 3 EVALUATION OF MASS AND SHAPE

### 3.1 Parameter identification procedure

The drag coefficient identification methodology is the same than [13], which is a previous work with the same facility. The general idea is to hover with the frame to characterize in front of a wind generator or wind tunnel. In this case, the wind is coming from a *WindShape* wind generator and the indoor position is provided by an *Optitrack* motion capture system. The Figure 2 shows the quadrotor during a calibration.

When the wind is blowing on a frame, the generated drag is balanced by the horizontal thrust coming from the bank

component	characteristic
material	aluminum & plastic (PLA)
motors	T-motor F30
propellers	Dalprop 5x4 (3 blades)
battery	3S, 2200 mAh
autopilot	Tawaki v1 with Paparazzi
GPS	U-blox M8
size (motor to motor)	47 cm
base mass	547 grams
additional masses	up to 520 grams
sphere diameter	22 cm
sphere mass	350 grams
flight time	7 to 15 minutes

Table 1: Quadrotor characteristics

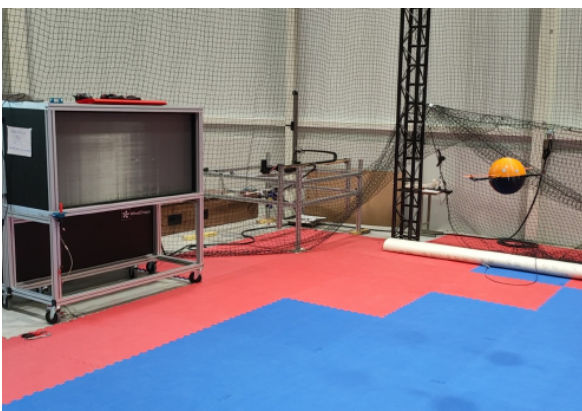


Figure 2: Quadrotor during calibration in front of the Wind-Shape wind generator.

angle. This angle is increasing with the wind speed. In order to mitigate errors due to attitude estimation offset, the frame is turning around its yaw axis. The result is that the roll and pitch angles, estimated by the Attitude and Heading Reference System (AHRS) from inertial measurements, are describing sinusoidal shapes. The Figure 3 is showing the roll angle during the calibration of the quadrotor. This flight correspond to four different wind speeds, with two complete turns of the frame at each speed. The red sine curves are fitted to the telemetry data. The magnitude of each oscillation corresponds to the bank angle of the quadrotor in the direction of the wind generator.

The conducted measurements are as follow:

- Five different quadrotor masses are tested: 0.547 kg (no additional mass), 0.677 kg, 0.807 kg, 0.937 kg and 1.067 kg
- For each mass, estimate bank angle at 9 different wind speeds from 2.5 m/s to 12.5 m/s
- Plot the tangent of the bank angle as function of speed for the different masses.

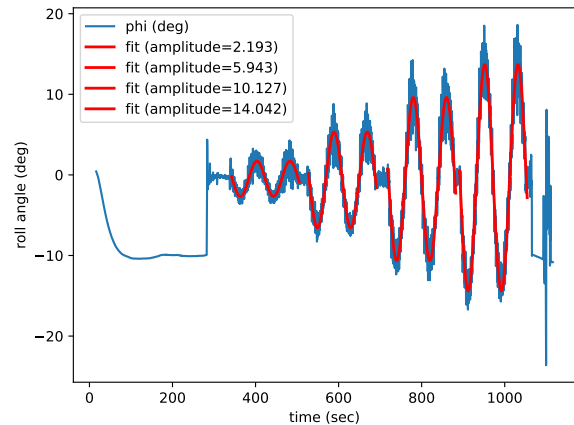


Figure 3: Estimation of the bank angle from sine curve fitting of the roll angle at different wind speed.

The result is shown in Figure 4. The next sections are analyzing the two most important outcomes of these data: the hypothesis of linearity of the drag model and the effect of the mass (and shape) on the drag coefficient.

### 3.2 Discussion on drag model

The Figure 4 is showing the mean bank angle as a function of wind speed for different mass configurations. It can be observed that between 2 m/s and 9 m/s, the relation between the angle and speed, thus between drag and speed, is linear. After that point, measurements are becoming unreliable due to important perturbations on the frame.

In [12], a similar result is found for a standard DJI quadrotor. At a bank angle of 6 deg, the drag switch from a linear to quadratic evolution, which correspond to an airspeed around 8 m/s to 10 m/s. Standard flight speed for such frame is around 5 m/s. In order to keep the model simple, we will assume that the relative airspeed on the frame stays lower to the critical speed, and only the linear part is considered.

The reference speed for each experiment have been established from the averaged measurements of an hot-wire anemometer. The comparison with other means of measurements (ultrasonic wind sensor) have shown that our reference probe might over estimate by 0.1 m/s to 0.5 m/s the speed. If corrected, the linear model holds down to a null speed.

### 3.3 Effect of mass and shape on drag

A first observation from Figure 4 is that at a given speed, the bank angle is decreasing with the added weight. This is also depicted in Figure 5. When the weight is increasing, the total thrust is increasing to compensate. The total drag is also increasing, however the bank angle is decreasing. This means that the drag is not increasing as fast as the weight.

Also from the data presented in Figure 4, linear regressions are applied on data lower than 9 m/s, for each of the

http://www.imavs.org/

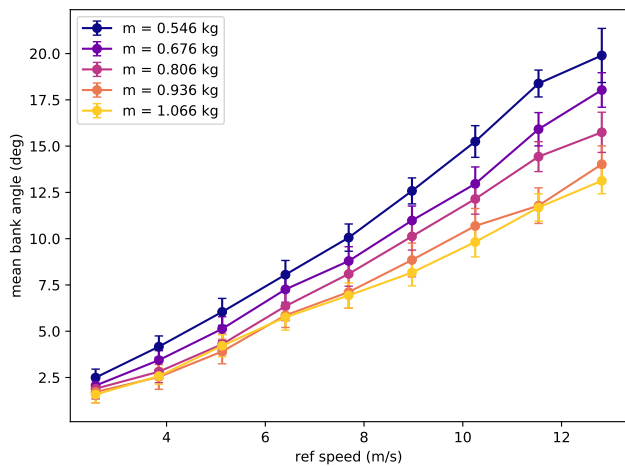


Figure 4: Mean bank angle at different wind speed and different masses; error bars are standard deviations on measurements

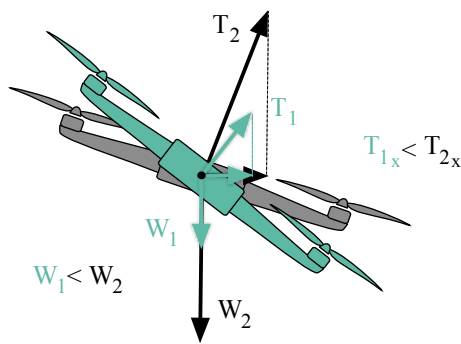


Figure 5: Thrust and weight forces applied on a quadrotor with two different mass. When the mass increases, the thrust increases to compensate the weight, the drag is also increased due to the increased motor speed, however, overall bank angle is reduced.

masses. Then the drag coefficient is computed as in [13]. The Figure 6 is showing the results by plotting the drag coefficients as a function of the mass of the quadrotor. Since the additional weight is not changing the overall shape, the variations of the drag is only related to the variations of motor speed, since a higher thrust is required with increasing weight. A linear regression is applied on the data, showing that the drag coefficient is increasing with the mass.

The influence of the shape is evaluated by comparing the drag coefficient of the quadrotor with and without the spherical body, at the same total weight. The green cross on Figure 6 (top right) is showing the drag coefficient with the sphere, coming from a previous calibration. It can be observed that the coefficient is much bigger, almost doubled by the presence of the large sphere at the center, which is an ex-

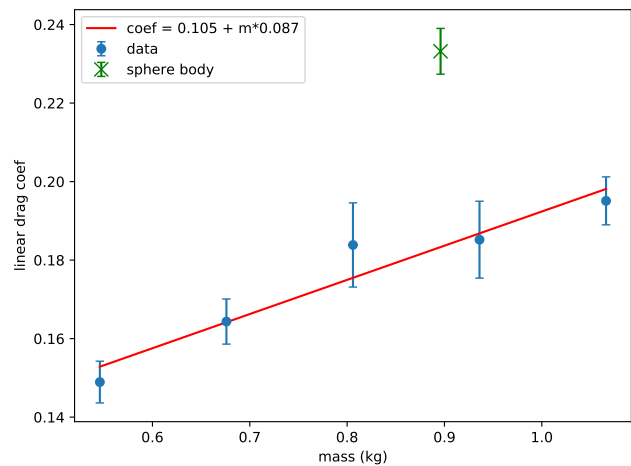


Figure 6: Linear drag coefficient as a function of mass; green cross indicates the model with spherical body; error bars are linear regression standard errors on linear regressions

pected result.

Finally, the Figure 7 is showing the drag coefficient over mass ratio ( $\frac{k}{m}$ ) as a function of the mass. This parameter is related to the sensitivity of the quadrotor to the wind. With higher ratio, the bank angle in hover is increasing at a given speed. As expected from previous curves, it is interesting to lower the mass while increasing the drag. In our case, the lightest frame without the sphere body is giving the best ratio (with the longest flight time as thrust is lower), even compared to the frame with the sphere body, generating more drag at the cost of an extra weight.

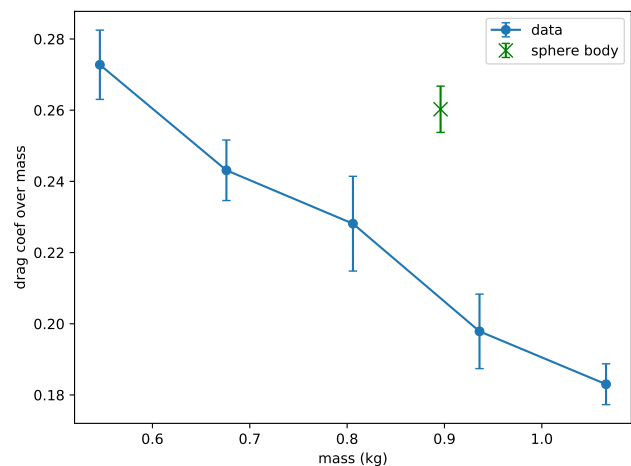


Figure 7: Linear drag coefficient over ratio as a function of mass; Green cross indicates the model with spherical body; error bars are linear regression standard errors on linear regressions

http://www.imavs.org/

#### 4 ESTIMATION OF DRAG FROM FLIGHT DATA

The previous section have shown that the weight and shape of the airframe have an important impact on the the drag coefficient. If it is possible to measure this value with a complex experimental setup involving wind tunnels, motion capture systems or forces and torque sensors, it would be more convenient to extract the relevant parameter from flight data directly. The next sections are presenting an approach to estimate the drag over mass  $\frac{k}{m}$  ratio from trajectory analysis using a least-square optimization method, followed by simulation and experimental results.

##### 4.1 Estimation using least-square optimization method

Least squares problems are optimization problems expressed in the form

$$\min_{x \in \mathbb{R}^n} \frac{1}{2} \|g(x)\|^2 = \frac{1}{2} g(x)^T g(x) = \frac{1}{2} \sum_{i=1}^m g_i(x)^2,$$

where  $g : \mathbb{R}^n \rightarrow \mathbb{R}^m$  is a differentiable function. In particular, these optimization problems arise when one wants to calibrate parameters of a mathematical model by using data. In our application, we are interested in analyzing the relationship between the drag coefficient thought  $k$  such that  $D = kV$  and the mass  $m$  of the quadrotor. It is postulated in [7] that, a simple dynamic particle model named “residual model” can be established in the following way :

$$f_{\epsilon}(k/m, \mathbf{W}) = \dot{\mathbf{V}}_{\mathbf{k}} - (\mathbf{T}_{spec} + \mathbf{D}_{spec}) \quad (7)$$

$$= \dot{\mathbf{V}}_{\mathbf{k}} - \left( \frac{mg\bar{\Theta}}{m} - \frac{k}{m} \mathbf{V}_{\mathbf{a}} \right) \quad (8)$$

$$= \dot{\mathbf{V}}_{\mathbf{k}} - \left( \mathbf{g}\bar{\Theta} - \frac{k}{m} (\mathbf{V}_{\mathbf{k}} - \mathbf{W}) \right) \quad (9)$$

where  $\mathbf{T}_{spec}$  and  $\mathbf{D}_{spec}$  are specific thrust and drag respectively, wind speed is  $\mathbf{W} = [W_x, W_y]^T$  and  $\bar{\Theta} = \tan(\Theta)$ . Thus, the specific coefficient ( $k/m$ ) and  $\mathbf{W}$  are unknown parameters to be determined. The least squares estimation of the unknown parameters is performed by solving the following optimization problem:

$$\min_{k/m, \mathbf{W}} \sum_{i=1}^m (\|f_{\epsilon}(k/m, \mathbf{W})\|)^2.$$

To find an approximation of a local minimum of the least squares problem, the *Scipy.optimize* package have been used. Several solvers are available for the `least_squares` interface. The two methods tested, *Trust Region Reflective* and *Levenberg-Marquardt* algorithms, are performing with similar results and resolution time.

##### 4.2 Simulation results

In order to evaluate the feasibility of the approach, it is first applied to simulation data. The simulator used is provided by the Paparazzi system and is based on the *JSBSim*

flight dynamic model. It can be considered as a high fidelity model that can take into account complex aerodynamic parameters and wind inputs. During the simulation, the mass is fixed to 0.897 kg and the drag coefficient to 0.230.

The trajectory of the quadrotor is a square with a side of 40 meters. Several simulated flights have been recorded at different wind speeds: 0 m/s, 4 m/s and 8 m/s, always coming from the North in NED frame. The commanded ground speed of quadrotor is 2 m/s. Similar results are obtained at 5 m/s, but are not presented here.

The Figure 8 presents the results of the simulation along the X axis (towards North), at the three different wind speeds. The data plotted correspond to the elements of the dynamic equation 7: acceleration, specific drag and specific thrust. The wind is correctly estimated in all cases with an error lower than 0.5 m/s in the worst case. The error (sum of the three aforementioned elements) is always close to zero. It is important to note that the data presented here are based on the perfect simulated values without sensor (IMU, GPS, barometer) noise nor bias.

The Table 2 is the synthesis of the simulation flights, presenting the estimated parameters compared to the values given as input to the simulator. It can be concluded that the method is functional and can provide excellent results on synthetic data.

#	mass sim (kg)	k sim	k/m sim	k/m estimated	W <sub>x</sub> est. (m/s)	W <sub>y</sub> est. (m/s)
1	0.897	0.23	0.256	0.257	-0.023	0.001
2	0.897	0.23	0.256	0.250	-4.13	0.039
3	0.897	0.23	0.256	0.245	-8.43	-0.006

Table 2: Simulation results for drag over mass coefficient and wind components for three different configurations: 1 - no wind, 2 - 4 m/s wind from North, 3 - 8 m/s wind from North. The commanded ground speed is 2 m/s. The drag and mass correspond to the quadrotor with sphere body. Corresponding acceleration and forces are shown on Figure 8

##### 4.3 Experimental flight results

In order to evaluate the method in realistic conditions, the same type of flight than in simulation have been performed with the real frame outdoor. These experimental flights were performed on a small airfield near Toulouse, using a standard GPS for positioning. The Figure 9 is the 3D trajectory of the quadrotor, in full autonomous navigation, at altitudes between 20 and 40 meters above ground.

On the day of the experiment, the average wind reported by public weather stations nearby was between 9 km/h to 11 km/h (2.5 m/s to 3 m/s) from the North (with a variation of  $\pm 20^\circ$ ). Unfortunately, the wind gust was also rather strong, from 5 m/s to 7 m/s.

http://www.imavs.org/

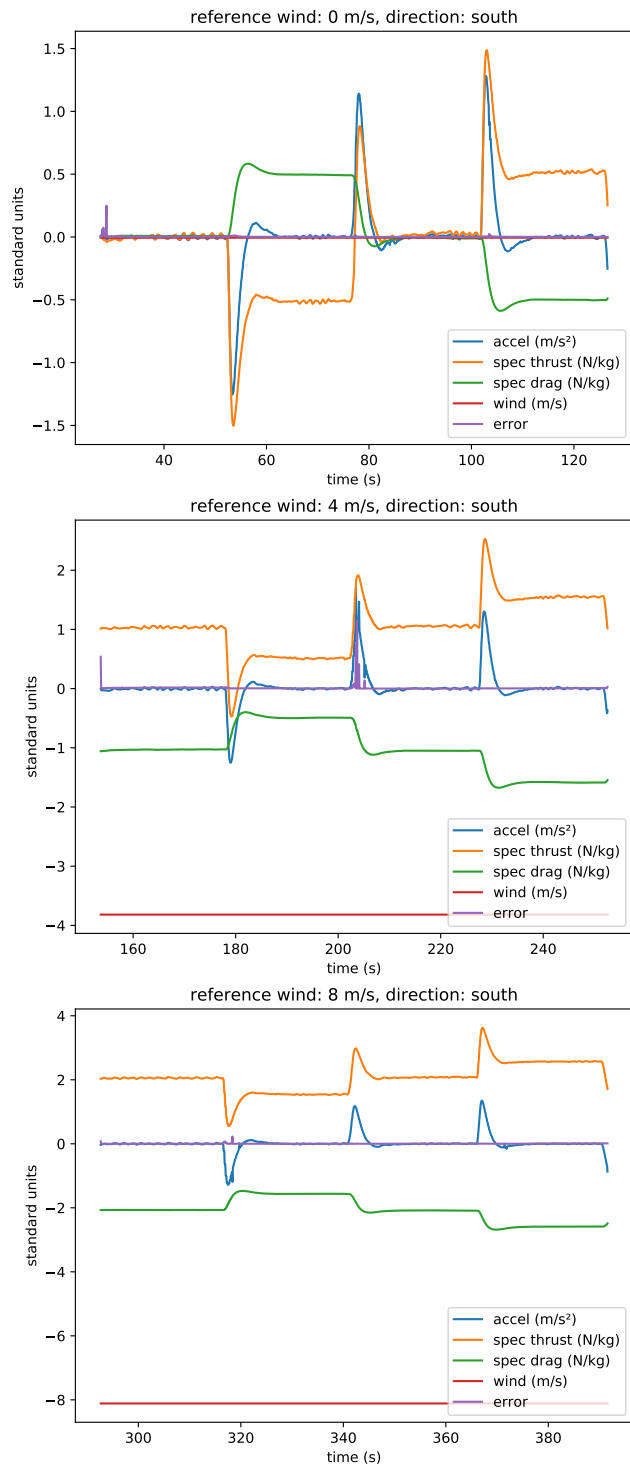


Figure 8: Evolution of acceleration, specific drag, specific thrust and equilibrium error during a square trajectory in simulation. Results are presented for the X axis only, at a wind speed of 0 m/s (top), 4 m/s (middle) and 8 m/s (bottom)



Figure 9: Square trajectory for outdoor experiment. The four segments are oriented North/South or West/East

Three different configuration of the quadrotor have been tested:

1. the light frame, with no additional mass
2. the heavy frame, with all the additional mass but with the same general shape than the light frame
3. the spherical body is placed around the electronics, resulting in a different shape but with almost the same weight than the heavy configuration

On the flight with the light configuration is detailed on Figure 10. Since the raw flight data are very noisy, they need to be filtered before applying the least-square optimization in order to obtain meaningful results. A Savitzky-Golay filter from the *scipy.signal* package is applied to all the input signals (ground speed and attitude angles) with the same parameters to avoid phase-shift issues. The acceleration is also obtained with this filter used as a differentiation filter on the ground speed. The first remark is on the wind estimate that seems to be very far from the expected value, in particular with a strong component towards the East. As mentioned before, the wind was rather turbulent on the day of experiment, and perceived direction and intensity by the operator (rather strong from NW) where actually closer to the estimated values than weather data.

The Figure 11 is specifically showing the residual error along the X and Y axis. This error is the sum of the acceleration minus the specific thrust and drag forces. As we can see, the fitting is rather good during the legs and constant speed, but the blue and orange curves are not matching well during the strong acceleration phases, corresponding to flight direction changes at each corner. A part of the problem might also come from the Savitzky-Golay filter smoothing the data.

http://www.imavs.org/

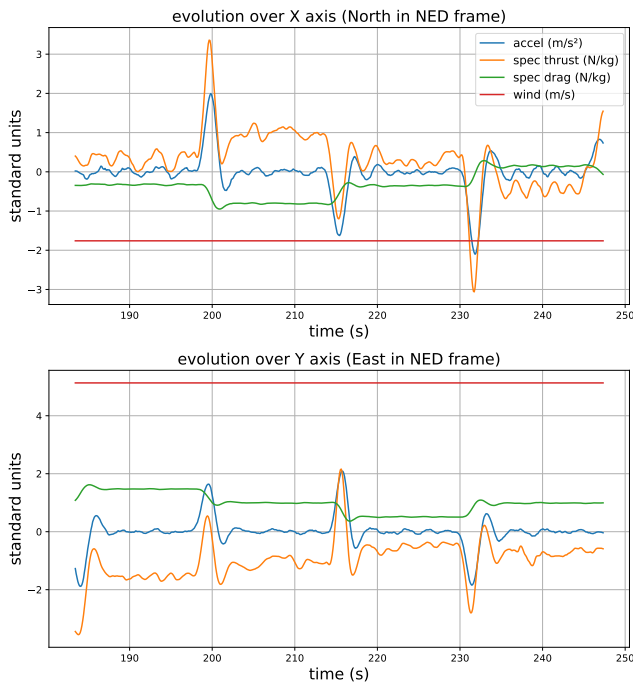


Figure 10: Evolution of acceleration, specific drag, specific thrust and estimated wind during a square trajectory in outdoor flight.

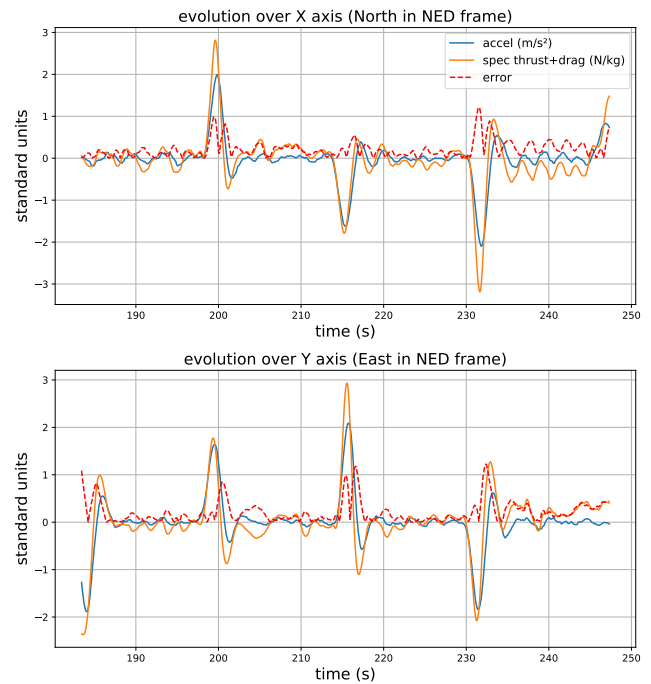


Figure 11: Evolution of equilibrium error during a square trajectory in outdoor flight.

The Table 3 is summarizing the outdoor experimental flights. Comparing the estimated and expected values, it is clear that this method, although giving realistic numbers, is not yet reaching the level of accuracy that one can expect for application to wind estimation.

Several hypothesis can be made to explain these bad results. First, the main assumption in the model is that the wind is constant, which was definitely not case during the experiment. Even if the flight had been performed to a calm day, a full square takes about 1 minutes. During that time, the wind is likely to have some gust. Reducing the flight time requires either a faster flight or a smaller square. The quadrotor will then face stronger or more frequent accelerations, which are the flight phases where the matching is the worst. The tests with a flight speed of 5 m/s (not presented) are producing even worse results.

Another possibility is that the pre-filtering method is not adapted and is introducing phase shift, although all data are filtered with the same parameters.

Finally, the input data, especially the attitude estimated from the onboard IMU, is very likely to have bias and delays compared to the perfect simulation data. Improving the state estimation filters should greatly improve the results.

### 5 CONCLUSION AND FUTURE WORK

The aim of this study was first to investigate the influence of mass and shape on the drag of a quadrotor, and second to

#	mass calib (kg)	k calib	k/m calib	k/m estimated	W <sub>x</sub> est. (m/s)	W <sub>y</sub> est. (m/s)
1	0.547	0.153	0.279	0.181	-1.44	2.84
2	0.867	0.180	0.208	0.0999	-5.71	1.56
3	0.897	0.230	0.256	0.157	-7.02	3.09

Table 3: Experimental results for drag over mass coefficient and wind components for three different configurations: 1 - light frame, 2 - heavy frame, 3 - spherical body

propose a method to estimate this drag coefficient from flight data. This parameter is crucial for wind estimation, but can also be used to improve the guidance and navigation. The conclusion for the tested model is that a light version is beneficial for the drag estimation. However, a shape generating drag is also interesting, thus a good compromise for a future experiment would be to find a structure generating drag at a low cost for the weight, for instance by using inflatable elements. Concerning the coefficient estimation, the method based on a least-square optimization, has proven to work in simulation but is facing difficulties with real flight data. There are several reasons for that, but the noise pre-filtering and the validity of assumption of constant wind during the complete procedure are most likely the critical points to address in a future work. For instance, the second point can be mitigated by flying early in the morning on a calm day, when there is almost no wind.

Another approach would be to integrate the drag coefficient to the state vector of a Kalman filter estimating the wind and airspeed. Compared to the work in [13], where the filter was a linear Kalman filter, introducing the drag coefficient would have two consequences: first the dynamic becomes non-linear, which requires an Extended Kalman filter formulation, and second the new state element is not always observable, it would depend on the current speed and acceleration of the system as discussed in [11]. Our goal for a future study is to establish the observability criteria so that the state, at least for the drag coefficient, is propagated only when observable and kept as a constant parameter otherwise. The main interest of a Kalman filter is that it can cope with variations of mass and shape during the flight without the need of specific calibration procedure. This could be applied for drones used in package delivery scenarios, while other methods are more adapted to frame with fixed characteristics such as the ones used for atmospheric science.

#### ACKNOWLEDGEMENTS

This work have been done using the preliminary work and calibration experiments of Victor Gravis, Théo Le Gall and Ziyad Baya, students at Enac, during their second year project under the supervision of the authors.

#### REFERENCES

- [1] Stéphanie Mayer, Gautier Hattenberger, Pascal Brisset, Marius Jonassen, and Joachim Reuder. A "no-flow-sensor" wind estimation algorithm for unmanned aerial systems. *International Journal of Micro Air Vehicles*, 4(1):pp 15–30, March 2012.
- [2] A. C. Kroonenberg, T. Martin, M. Buschmann, J. Bange, and P. Vörsmann. Measuring the wind vector using the autonomous mini aerial vehicle m2av. *Journal of Atmospheric and Oceanic Technology*, 25:1969–1982, 2008.
- [3] S. Prudden, A. Fisher, M. Marino, A. Mohamed, S. Watkins, and G. Wild. Measuring wind with small unmanned aircraft systems. *Journal of Wind Engineering and Industrial Aerodynamics*, 176:197–210, 2018.
- [4] Jean-Philippe Condomines, Murat Bronz, Gautier Hattenberger, and Jean-François Erdelyi. Experimental Wind Field Estimation and Aircraft Identification. In *IMAV 2015: International Micro Air Vehicles Conference and Flight Competition*, Aachen, Germany, September 2015.
- [5] Carl A. Wolf, Richard P. Hardis, Steven D. Woodrum, Richard S. Galan, Hunter S. Wichelt, Michael C. Metzger, Nicola Bezzo, Gregory C. Lewin, and Stephan F.J. de Wekker. Wind data collection techniques on a multi-rotor platform. In *2017 Systems and Information Engineering Design Symposium (SIEDS)*, pages 32–37, 2017.
- [6] Fabrizio Schiano, Javier Alonso-Mora, Konrad Rudin, Paul Beardsley, Roland Siegwart, and Bruno Sicilianok. Towards estimation and correction of wind effects on a quadrotor uav. In *IMAV 2014 : International Micro Air Vehicle Conference and Competition 2014*, pages 134 – 141, Delft, 2014. International Micro Air Vehicle Conference and Competition 2014 (IMAV 2014). International Micro Air Vehicle Conference and Competition 2014 (IMAV 2014); Conference Location: Delft, Netherlands; Conference Date: August 12-15, 2014.
- [7] Javier González-Rocha, Craig A. Woolsey, Cornel Sultan, and Stephan F. J. De Wekker. Sensing wind from quadrotor motion. *Journal of Guidance, Control, and Dynamics*, 42(4):836–852, 2019.
- [8] L.N.C. Sikkkel, G.C.H.E. de Croon, C. De Wagter, and Q.P. Chu. A novel online model-based wind estimation approach for quadrotor micro air vehicles using low cost mems imus. In *2016 IEEE/RSJ International Conference on Intelligent Robots and Systems (IROS)*, pages 2141–2146, 2016.
- [9] Patrick P. Neumann and Matthias Bartholmai. Real-time wind estimation on a micro unmanned aerial vehicle using its inertial measurement unit. *Sensors and Actuators A: Physical*, 235:300–310, 2015.
- [10] Matthew Marino, Alex Fisher, Reece Clothier, Simon Watkins, Samuel Prudden, and Chung Sing Leung. An evaluation of multi-rotor unmanned aircraft as flying wind sensors. *International Journal of Micro Air Vehicles*, 7(3):285–299, 2015.
- [11] Robert C. Leishman, John C. Macdonald, Randal W. Beard, and Timothy W. McLain. Quadrotors and accelerometers: State estimation with an improved dynamic model. *IEEE Control Systems Magazine*, 34(1):28–41, 2014.
- [12] Kilian Meier, Richard Hann, Jan Skaloud, and Arthur Garreau. Wind estimation with multirotor uavs. *Atmosphere*, 13(4), 2022.
- [13] Gautier Hattenberger, Murat Bronz, and Jean-Philippe Condomines. Estimating wind using a quadrotor. *International Journal of Micro Air Vehicles*, 14:17568293211070824, 2022.
- [14] Gautier Hattenberger, Murat Bronz, and Michel Gorraz. Using the Paparazzi UAV System for Scientific Research. In *IMAV 2014, International Micro Air Vehicle Conference and Competition 2014*, pages pp 247–252, Delft, Netherlands, August 2014.